The Ductile–Brittle Transition in Macroscopic Tensile Tests on Polyethersulfone

C. J. G. PLUMMER and A. M. DONALD, *Cavendish Laboratory, Cambridge University Department of Physics, Madingley Road, Cambridge CB3 0HE, United Kingdom*

Synopsis

In tensile tests of polyethersulfone it is found that, as the temperature is raised, samples of low molecular weight exhibit a ductile–brittle transition. Thus, this normally tough polymer becomes less so at evaluated temperatures. Ultimately as the temperature is raised to close to T_g, more ductile behavior returns as homogeneous deformation occurs. For high molecular weight samples, at the strain rates used ($\sim 10^{-4}$ s^{-1}) ductile behavior was found at all temperatures with a neck forming as deformation proceeds. These findings can be rationalized in terms of a disentanglement model for craze formation: crazing via a disentanglement mechanism will be favoured by low molecular weight and high temperature, thus allowing craze-initiated fracture to intervene before shear deformation has taken place. A comparison is made both with earlier work on thin films of polyethersulfone and with a theoretical model.

INTRODUCTION

Polyethersulfone (PES) is an amorphous high entanglement density thermoplastic with a glass transition temperature T_g of approximately 220°C, and the structure

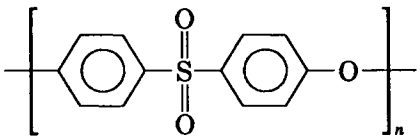

The high T_g of PES makes it of potential use in applications demanding high service temperatures and long term durability. However, when contemplating such applications it is important to have a knowledge and understanding of the circumstances under which the ductile behavior generally observed in mechanical tests on PES at ambient temperature may be replaced by brittle failure, this latter being undesirable from an engineering standpoint.

In view of the known embrittling effect of crazing on glassy polymers, we have been prompted to investigate the possibility of a transition from shear deformation to crazing in PES with increasing temperature. From microscopic studies of thin films of high entanglement density glassy polymers, including PES, deformed at various temperatures we showed that such transitions do take place.[1] As indicated in Figure 1 for PES, it was found that typically the onset of crazing was characterized by a steep drop in the strain to craze with temperature. Furthermore, we found that in this transition region the strain

Journal of Applied Polymer Science, Vol. 41, 1197–1212 (1990)
© 1990 John Wiley & Sons, Inc. CCC 0021-8995/90/5-61197-16$04.00

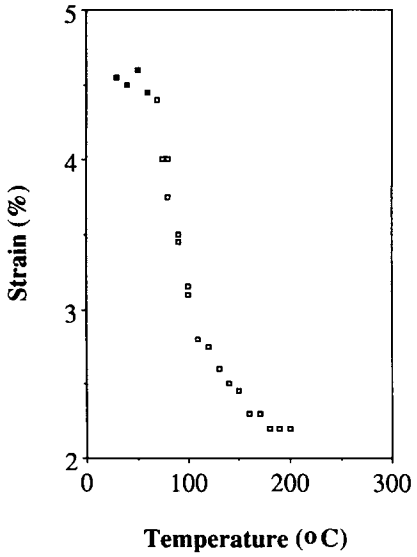

Fig. 1. The strain for deformation onset as a function of temperature in thin films of PES aged for 70 hours at 200°C and strained at a strain rate of 10^{-2} s^{-1}. Filled symbols represent shear deformation and open symbols represent crazes.

to craze fell with decreasing molecular weight and showed a much stronger dependence on deformation rate than did the yield strain.[1]

Such a molecular weight dependence is suggestive of a disentanglement mechanism. Disentanglement may be visualized as the escape of a given chain from a notional tube representing the entanglement constraint, or effectively the topological constraint on relative chain motion arising from nearest neighbor interactions.[2,3] Since, in general, one would expect such a mechanism to be both strongly thermally activated, and associated with a relatively long characteristic time (since it involves the motion of whole chains), we have argued that disentanglement crazing should be favored over shear deformation by high temperatures and long times, consistent with our observations.[1] More recently some success has been achieved in developing semiquantitative models for disentanglement crazing.[4,5] The underlying concept in these models is that of "forced" reptation, in which a polymer chain is pulled from its confining tube under the influence of an external stress (as distinct from "classical" reptation which refers to Brownian motion).[4]

The propagation rate of a craze may be argued to be determined by the rate at which it widens, and observations of crazing in a variety of polymers show that crazes widen by a surface drawing mechanism.[6,7] Kramer has shown that if one assumes the widening rate to be governed by the flow of polymer in a thin, strain-softened layer at the bulk–polymer interface along the gradient in hydrostatic tension between the void tips and the fibril bases, then

$$S_c \sim F(T, \dot{\epsilon})\Gamma^{1/2} \tag{1}$$

In this equation S_c is the crazing stress, $F(T, \dot{\epsilon})$ is a front factor related to the

constitutive behaviour of the strain softened layer and weakly dependent on the temperature T and deformation rate $\dot{\epsilon}$, and Γ is the effective surface energy at the void tips.[6] As may be seen from Figure 2, in order for chains to be free to move into the newly forming craze fibrils they must either be able to move relative to their confining tubes embedded in the bulk (disentanglement), or undergo chain scission in the neighourhood of the void tip. In either case, one may model the effect of this geometrically necessary entanglement loss in terms of an increment in the surface tension at the void tip.[6] In order for the void tip to advance, not only must the van der Waals interactions between chains be overcome, but also the extra forces required to overcome the entanglement constraint. Based on the approach of Kramer and Berger,[5] we obtain the following expressions (see Appendix A):

$$S_c \sim \left(\Gamma_0 + (1 - x_c)\frac{d\nu_e U}{4}\right)^{1/2} \qquad \tfrac{1}{2} > x_c \tag{2a}$$

$$S_c \sim \left(\Gamma_0 + \frac{1}{4x_c}\frac{d\nu_e U}{4}\right)^{1/2} \qquad \tfrac{1}{2} \leq x_c \tag{2b}$$

where

$$x_c = \frac{U}{4a}\frac{M_0}{\zeta_0 \upsilon M} \tag{2c}$$

(U is the bond energy, ν_e is the entanglement density, d is the entanglement separation, a is the length of a covalent bond in the chain backbone, Γ_0 is the van der Waals surface energy, ζ_0 is the monomeric friction coefficient, M_0 is the monomer molecular weight, and υ is the craze widening rate, which we assume to be proportional to $\dot{\epsilon}$.) Denoting x as the proportion of the length of a given chain which must disentangle in order for crazing to proceed, then x_c represents a critical value of x. If $x > x_c$ then the force to disentangle, which is proportional to x, will be greater than the force to break the chain and so one expects chain scission to occur. Since x may take any value between 0 and $\frac{1}{2}$ for individual chains, then for $x_c < \frac{1}{2}$ entanglement loss is accommodated

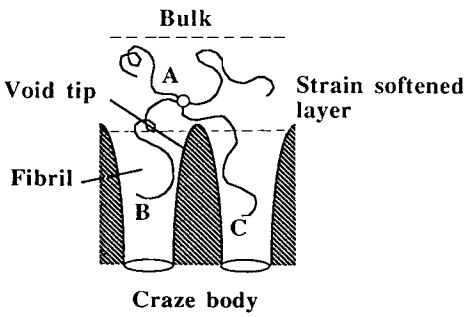

Fig. 2. A schematic representation of entanglement loss during craze widening. The chains marked B and C and entangled at A must either disentangle or break in order to move into adjacent fibrils.

both by scission and disentanglement and, in the limit of x_c tending to zero, disentanglement is replaced entirely by scission so that

$$S_c \sim \left(\Gamma_0 + \frac{d\nu_e U}{4}\right)^{1/2} \tag{3}$$

This equation is that originally proposed by Kramer[6] to describe crazing in high molecular weight, low ν_e polymers such as polystyrene (PS) at ambient temperature, under which conditions we expect x_c to be small (since both M and ζ_0 are relatively large).

In high ν_e polymers such as PES, the second term in eq. (3) is very much greater than in low entanglement density polymers, so that when x_c is small, S_c is higher than the yield stress and shear deformation replaces scission crazing as the dominant deformation mechanism. Since the temperature dependence of scission crazing is expected to be weaker than that of the yield stress,[8,9] we may therefore argue that any transition from shear to crazing in PES must be associated with the onset of disentanglement controlled crazing. Similar explanations have been put forward to explain the phenomenology of crazing in polycarbonate (PC)[1,6] and low molecular weight PS close to T_g.[5,8,9]

That disentanglement crazing should be favored by high temperatures is a consequence of the strong temperature dependence of ζ_0. Since ζ_0 is related to the inverse of the segmental mobility, we expect it to scale as $\exp(\Delta H/RT)$, where ΔH is the activation energy for the segmental mobility.[4] (Measurements of the melt viscosity in PES[10] suggest ΔH to be approximately 115 kJ mol^{-1}.) As the mobility of the chains increases we expect a cross-over from the scission dominated regime to the entanglement dominated regime where $x_c = \frac{1}{2}$. (It should be noted that although eq. (2c) implies that x_c can take values greater than $\frac{1}{2}$, of course this has no physical meaning and the whole chain can be regarded as being mobilized in this case.) For example as indicated in Figure 1, the transition from shear to crazing in thin films of low molecular weight average PES (approximately 47,000) and the associated steep drop in crazing strain, occur at approximately 80°C for $\dot{\epsilon} = 10^{-2}$ s^{-1}. Close to T_g we expect the chain mobility to be sufficiently large that the contribution to Γ from entanglement loss is negligible and the crazing stress S_c is dominated by Γ_0. Since Γ_0 is not strongly dependent on either temperature or strain rate, the temperature and strain rate dependences of S_c in this "van der Waals" regime are weak. Similarly, there should be no molecular weight dependence of S_c, which is consistent with the observation that the strain to craze against temperature curves for the various molecular weight averages in Figure 1 converge as T approaches T_g (see also Fig. 3 in Ref. 1).

On a macroscopic scale, ductile-brittle transitions have been identified in fatigue, creep rupture, and impact tests on PES by Davies et al.[11] In particular they found that whereas PES remained ductile during creep rupture measurements made at ambient temperature, there was a pronounced ductile-brittle transition when similar measurements were carried out at 150°C. It was suggested by Davies et al. that this could be linked to a disentanglement mechanism. In the remainder of this paper we shall look at the extent to which the phenomenology of crazing in thin films of PES[1] and the theory which has been

developed to account for the possibility of disentanglement crazing[4,5,9] are consistent with the behaviour of macroscopic test samples. In order to do this we look at the simple case of tensile tests on unnotched test bars. We have sought to confirm the existence of a ductile-brittle transition in PES with increasing temperature for this geometry, and to link the observations with our model for crazing in PES.

EXPERIMENTAL

The samples used were VICTREX PES tensile test bars with 12.7 × 3.2 mm cross sections, kindly supplied by ICI plc. They were manufactured from four different grades, with molecular weight averages of 47,000, 52,000, 58,000, and 63,000, which we refer to here as M_w1, M_w2, M_w3, and M_w4, respectively, and polydispersities of the order of 2 (more details of the molecular weight distributions are given in Ref. 11). All the samples were initially dried under vacuum at 100°C to remove excess water. Some of the samples were then given a further 70 h aging treatment at 180°C, since from our previous work we expected this to raise the yield stress and hence extend the temperature range in which crazing could be observed.

The tests were carried out in the environmental chamber of an Instron tensile test machine at a constant cross-head displacement rate of 1 mm/min. Stress–strain curves were recorded for various temperatures for each grade and subsequent to testing, optical microscopy on a Carl Zeiss Jenapol microscope was carried out.

RESULTS

Depending on the sample type and test conditions, one of two distinct deformation and failure mechanisms was observed in the macroscopic tests—ductile and brittle. We shall first discuss what we term ductile behavior, that is, either localized shear necking or uniform thinning via shear of the samples. Such ductility was shown by the highest molecular weight over the entire temperature range, and by the other samples over an increasingly limited temperature range as the molecular weight was decreased. Aging also tended to decrease the temperature range over which ductile behavior was observed.

Examination of the samples subsequent to deformation showed that in the regime of ductile behavior characterized by localized necking, the necks had formed with an extension ratio of approximately 1.4 in all cases (as measured by comparing cross-sectional areas of the sample before and after necking). Although extension ratios became more difficult to measure as the temperature was increased, since the extent of necking became severely limited owing to fracture intervening, no systematic change in extension ratio with temperature was observed. However, there was a tendency for the necks to become less sharply defined at high temperature. Indeed, where ductile behavior persisted up to temperatures close to T_g, homogeneous deformation and uniform thinning eventually replaced necking. Figure 3 shows the nominal stress-strain curves at various temperatures corresponding to ductile behavior in aged PES M_w4. It may be seen from the figure that at temperatures close to ambient temperature the stress–strain curves showed a sharp yield drop. However, as the temperature increased, the stress drop beyond the upper yield point became smaller, even-

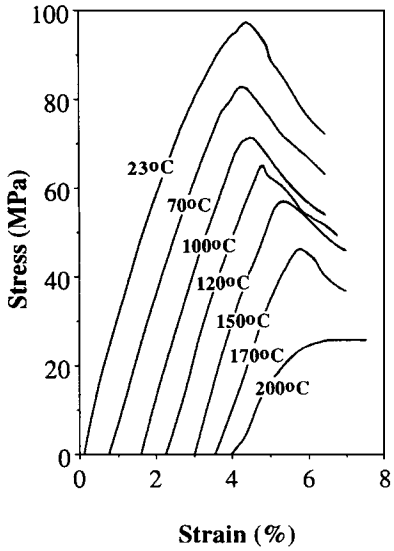

Fig. 3. Nominal stress–strain curves for aged PES M_w4 at various temperatures.

tually disappearing close to T_g in which regime we observed homogeneous deformation throughout the sample.

Widespread crazing could be observed in high molecular weight samples at relatively high temperatures, but close examination of these crazes showed that

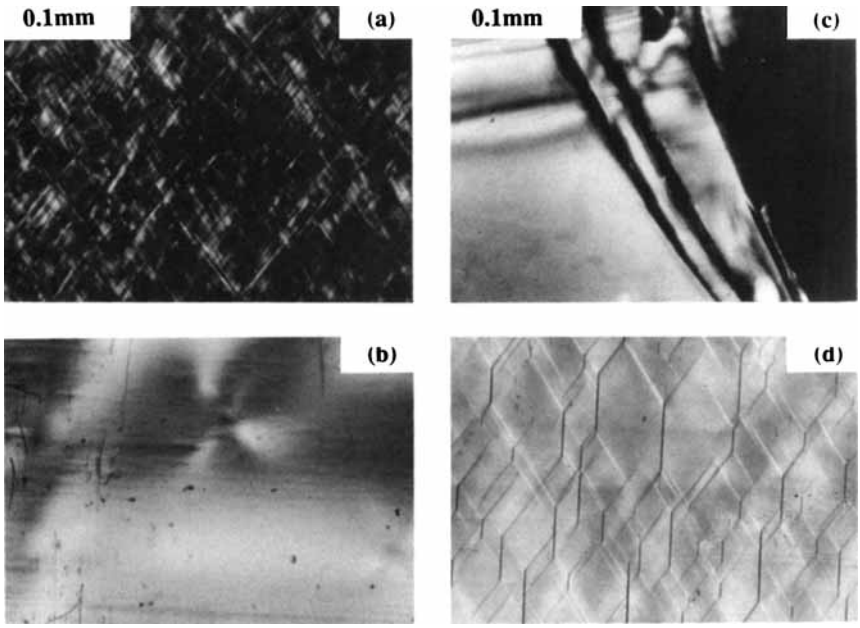

Fig. 4. Optical micrographs of deformation in PES: (a) microshear bands in PES M_w4 at 140°C viewed under cross polarizers; (b) microshear bands in PES M_w4 at 40°C viewed under crossed polarizers; (c) large crazes adjacent to the fracture surface in PES M_w1 at 140°C; (d) shear blunting of crazes in PES M_w4 at 170°C viewed under crossed polarizers.

they had for the most part nucleated at the sample surface, and been prevented from growing more than about 0.1 mm in length owing to shear blunting at the craze tips [Fig. 4(d)]. In samples where such crazes were observed, fracture tended to occur subsequent to neck formation and the cracks nucleated within the necks. At the highest temperatures, when homogeneous deformation was occurring, there were essentially no crazes.

The onset of bulk shear deformation was characterized by the appearance of an angled neck oriented at approximately 55° to the tensile axis (this orientation is a consequence of the unequal constraints on deformation of a rectangular cross section). As the necks grew they gradually changed their orientation because of changes in the geometrical constraints, so that in cases where the neck could be grown to a length of a few centimeters, the neck shoulders eventually became perpendicular to the tensile axis.

In the macroscopic tests considerable stress whitening was observed in association with yielding. This was thought to arise in part from a residual water content which may lead to the nucleation of small bubbles in deformed regions of the sample (similar whitening may occur when the temperature of the samples is raised rapidly by, for example, exposure to a candle flame). The extent of this phenomenon could be reduced by prolonging the drying time, but some whitening remained.

The second contributing factor was associated with the presence of extremely high densities of well defined micro-shear bands oriented at approximately 45° to the tensile axis. These are shown in Figure 4(a). They could be observed principally in the regions of the sample adjacent to the necks, but also to a lesser extent in the necks themselves. In aged samples showing ductile behaviour, the shear bands became very densely packed at intermediate temperatures, reaching a maximum density in the temperature range 140°–180°C. Close to T_g and close to ambient temperature, the shear bands were much coarser and only detectable as local changes in birefringence when the deformed samples were viewed under crossed polarizers [Fig. 4(b)], since they were diffuse. Other polymers, such as PS, also show a tendency for diffuse band formation as the temperature approaches T_g, as discussed by Bowden.[12] However, it is not immediately clear why the bands should also be diffuse in appearance near ambient temperature. At low temperatures the neck often shows a transverse displacement at either side, and the angle of inclination is somewhat variable, both characteristics of a hybrid tensile-shear deformation as discussed by Bowden.[12] Unaged samples showed very little shear banding over the whole temperature range, although, again, it was most noticeable at intermediate temperatures.

Turning now to brittle fracture, in the low and intermediate molecular weight samples as the temperature was increased there was a tendency for brittle fracture to replace ductile yielding as the principal mode of deformation. Brittle fracture initially (i.e., at low temperature) occurred as a post yield phenomenon, as shown in Figure 5; this figure gives stress–strain curves for PES M_w1. However, the observed rapid decrease with temperature in the stress to fracture meant that over the bulk of the temperature regime in which brittle fracture took place, it occurred in the linear region of the stress–strain curve. This is also shown in Figure 5. Under these circumstances no necking or shear banding was observed, and the fracture surface and regions of the sample immediately adjacent to the fracture plane were characterized by large crazes. Such crazes

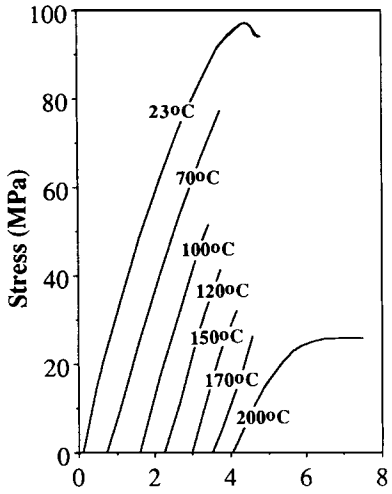

Fig. 5. Nominal stress–strain curves for aged PES M_w1 at various temperatures.

are shown in Figure 4(c). For intermediate temperatures there was no crazing in the bulk of the sample. At temperatures very close to T_g (above 200°C) there was a tendency for a return to ductile behavior. The ductility at these temperatures was no longer associated with necking but with homogeneous deformation, and there was no pronounced yield drop in the stress–strain curves.

DISCUSSION

Data for the stress for deformation onset against temperature for the various samples are summarized in Figures 6 and 7. Figure 6 shows the variation in

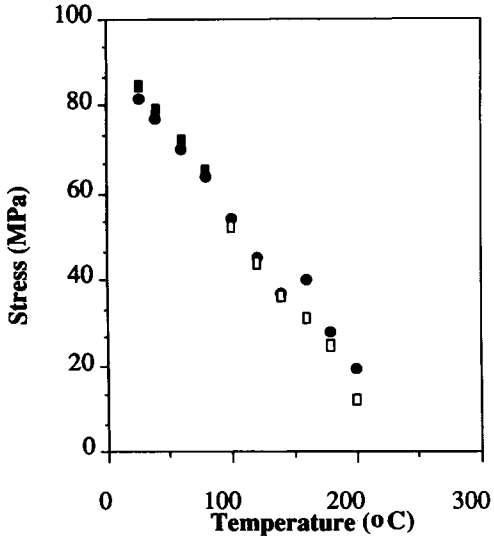

Fig. 6. The deformation stress as a function of temperature for unaged PES M_w1 and PES M_w4. The data points represent the maximum stress reached during deformation: (●) M_w4—ductile necking; (■) M_w1—ductile necking; (□) M_w1—brittle fracture without necking.

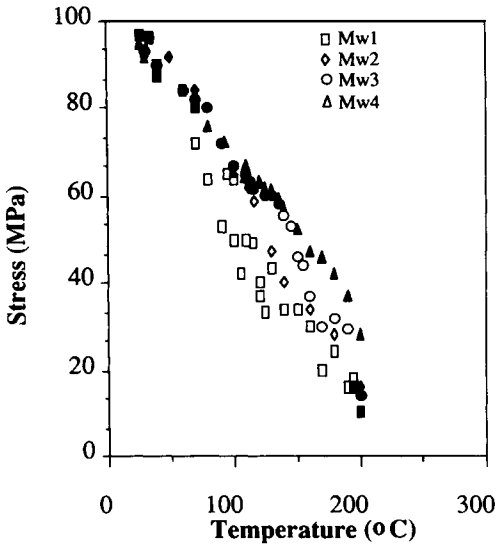

Fig. 7. The deformation stress as a function of temperature for all four grades of PES investigated, aged for 70 h. Filled symbols represent ductile necking and open symbols represent brittle fracture without necking.

the deformation stress as a function of temperature for unaged PES M_w1 and PES M_w4. The data points represent the maximum stress reached during deformation. In the case of a yield drop and consequent necking, this corresponds to the upper yield stress. Where brittle fracture occurred prior to the yield drop, it corresponds to a fracture stress as indicated in the figure. Figure 7 shows the stress for deformation onset against temperature for all four grades, aged for 70 h. It may be readily seen that there was indeed a transition from ductile to brittle behavior with increasing temperature, particularly in the low molecular grades (for this aging treatment and strain rate the highest molecular weight PES M_w4 remained ductile over the whole temperature range). As comparison of Figures 6 and 7 shows, the yield stress was raised by aging for 70 h at 180°C whereas the stress for brittle fracture remained unaffected, consistent with our observation that the crazing strain is independent of aging in thin films.[1] Furthermore, although the fracture stress decreased with molecular weight just above the ductile–brittle transition, as T approached T_g, the fracture stresses for the different molecular weights converged, again, consistent with the behavior of the crazing strain in thin films.

Other parallels with the behaviour of the thin films can also be found. As mentioned above, the extension ratio within necks was found to be 1.4. This value is consistent both with extension ratios measured in deformation zones (DZs)[1] in thin films of PES (DZs are regions of local shear necking, cracklike in shape, which run perpendicular to the direction of the applied stress in thin films) and with estimates of the natural draw ratio from molecular parameters and rheological data (see Appendix B). Furthermore, the change in neck shape with temperature also correlates with the behavior of the DZs. In aged thin films of PES it was found[1] that, although DZs in PES were sharply defined at room temperature, the change in film thickness at the edges of the DZ s became

more gradual as the temperature was increased. This effect is demonstrated in Figure 8, which shows microdensitometer scans of transmission electron micrograph negatives taken across (i.e., perpendicular to the length of) two DZs at 20 and 80°C. The microdensitometer measures the optical density of the negative, and therefore these traces are a direct measure of the local extension ratio, via a logarithmic transformation.[13] The decrease in optical density (and therefore increase in extension ratio) is much sharper at the lower temperature. (Similar behavior has been reported for thin films of crosslinked PS.[14]) Very close to T_g no localized features were observed when the thin films were deformed and it is assumed that they were undergoing homogeneous deformation as in the macroscopic tests. In the absence of an aging treatment, freshly formed thin films showed a much diminished tendency for localized deformation, and DZs were replaced by diffuse shear patches.

The absence of widespread crazing in cases where brittle fracture was observed prior to yield suggests that brittle fracture corresponds closely with the crazing stress in such instances. Since in the macroscopic samples, brittle fracture occurred for the most part in the linear region of the stress–strain curve, it suggests that we are justified in assuming that the crazing strain in the thin films is linearly related to the crazing stress. (In the case of the onset of shear necking, that is, the appearance of shear deformation zones in the thin films, this assumption is clearly no longer valid. Necking occurs beyond the yield drop and the stress–strain curves show varying degrees of curvature in this region as can be seen in Figure 3, so that the strain to form a deformation zone is only a rough guide to the behavior of the yield stress.)

It can be argued that the failure stress will coincide with the crazing stress from a fracture mechanics point of view. One approach[15] is to assume that the presence of a craze at a crack tip may be modelled by assuming a cohesive stress, equal to the crazing stress S_c, to act perpendicular to a line zone extending

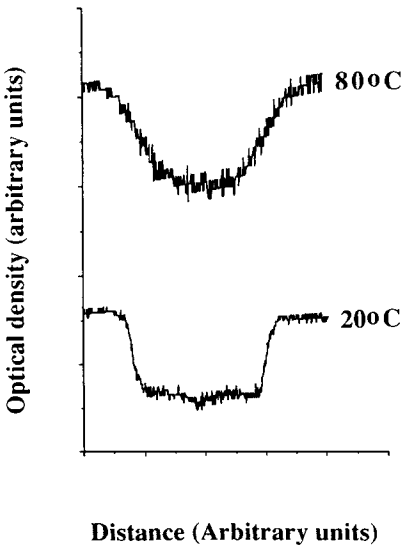

Fig. 8. Microdensitometer profiles of TEM negatives of DZs in thin films of PES M_w4 at various temperatures showing the variation in extension ratio across the width of the DZs.

a distance r_c beyond the crack tip. If the bulk polymer may be treated as linear elastic, then if S_f is the fracture stress

$$\frac{r_c}{a} = \ln \sec \frac{\pi}{2} \frac{S_f}{S_c}$$

where

$$r_c = \frac{\pi}{8} \frac{EJ}{S_c^2} \tag{4}$$

a is the crack length, E is the Young's modulus, and J is a critical energy release rate fracture criterion. It is easy to show that, for a/r_c less than 0.2, the fracture stress S_f becomes very close to the crazing stress. Thus, for unnotched specimens, such as ours, the failure stress should approximate well to the crazing stress. Experiments on crazing and fracture in PMMA appear to confirm this,[14] and certainly the form of the curves of Figures 6 and 7 for the low molecular weight PES seem consistent with our thin film results in Figure 1.

We now wish to see how far the understanding gained from the thin film studies previously made can be employed in interpreting the macroscopic data. In order to investigate this more quantitatively, we have converted our strain to craze results for the thin films into stresses using measurements of Young's modulus as a function of temperature. These measurements were obtained from the macroscopic tests and are shown in Figure 9. Before a comparison can be made with the thin film data, allowance has also to be made for the different strain rates used in the two types of experiment. (The effective strain rate in

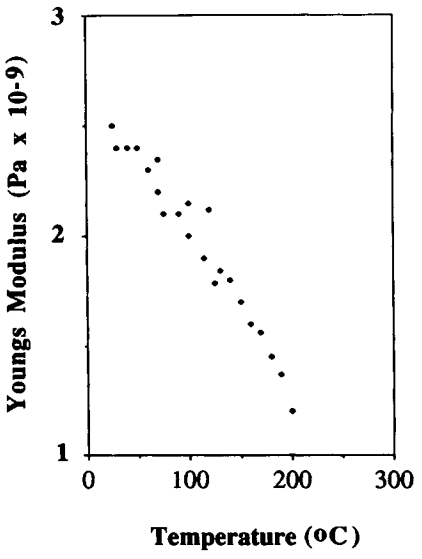

Fig. 9. The observed variation of Young's modulus as a function of temperature in PES. The Young's modulus is estimated from the slope of the tangent to the nominal stress–strain curves at a stress of 20 MPa.

the macroscopic tests was approximately 2×10^{-4} s^{-1}, and in the thin film work 10^{-2} s^{-1} for the data in Figure 1. Some additional data were also collected at 6×10^{-5} s^{-1}.) To effect this, we have looked at the extent to which the strain rate scaling suggested by eq. (2) is consistent with the two sets of data by making specific allowance for a front factor which is dependent on both temperature and strain rate.

Equation (2a) can therefore be written:

$$S_c = F(\dot{\epsilon}, T)\left(\Gamma_0 + (1 - x_c)\frac{d\nu_e U}{4}\right)^{1/2}, \quad \tfrac{1}{2} > x_c$$

and similarly eq. (2b). Assuming ν_e to be 50×10^{25} m^{-2} and d_e to be 3.2 nm (see Appendix B), and U to be 6×10^{-19}, J, we estimate the quantity $d\nu_e U/4$ to be approximately 0.24 J m^{-1} compared with a value for Γ_0 of approximately 0.04 J m^{-2} (estimates of U and Γ_0 are from Ref. 6).

It is now assumed that the front factor is separable into terms dependent on T and $\dot{\epsilon}$ only, so that $F(\dot{\epsilon}, T) = G(\dot{\epsilon})H(T)$. We assume that the overall effect of all the factors contributing to F is to give a linear variation of $H(T)$ with T (from observations of the stress to craze in PS[9], this is not unreasonable). x_c itself has an exponential temperature dependence, through the parameter ζ_0, the chain mobility. Equation (2c) gives x_c as $(U/4a)$ $(M_0/\zeta_0 \upsilon M)$ which, since we are assuming υ is proportional to $\dot{\epsilon}$, can be written as $A \exp(\Delta H/RT)$, with A inversely proportional to $\dot{\epsilon}$ and M. A will be taken as an adjustable parameter in making the fits of the experimental data to eqs. (2a) and (2b). From the work of James[10] ΔH is found to be 115 kJ mol^{-1}. Since the shear-to-craze transition must occur where the two surface energy terms in eq. (2) are comparable, that is, at about 90°C, this suggests that (for this value of ΔH) the van der Waals regime where the crazing stress is determined only by Γ_0, occurs at 130°C and above for a strain rate of 10^{-2} s^{-1}. Above 130°C then, all the temperature variation is taken up by $H(T)$. Thus by fitting the observed linear dependence in this temperature regime we obtain an empirical form for $H(T)$. We assume that this form for $H(T)$ can be extrapolated to lower temperatures.

From Kramer's discussion of the widening rate law for PS,[6] it seems reasonable to assume a power law variation of G with $\dot{\epsilon}$. (Explicitly Kramer gives $G \sim \dot{\epsilon}^{1/2n}$ with $10 < n < 20$.) In so doing we are implicitly ignoring variations in the Young's modulus with strain rate, since this has only been measured at one strain rate, but is being used to convert all the thin film data to stresses. Considering the data for PES strained at 6×10^{-5} s^{-1}, and assuming $H(T)$ is unchanged, we find a strain rate scaling for $G(\dot{\epsilon})$ consistent with an n of approximately 16, and a reasonable fit to the high temperature data.

At this point we can specify the front factor at any temperature and strain rate, using three parameters: n and the two parameters required to give the linear dependence of $H(T)$. Given this, the data for the stress to craze in the vicinity of the shear to craze transition can be fitted by varying A. This has been done for the data gathered at a strain rate of 10^{-2} s^{-1}. This value of A can then be scaled (being inversely proportional to strain rate) to generate predicted curves for the other two strain rates (after allowance has been made

for the power law strain rate dependence of G). These curves are all shown in Figure 10, together with the experimental data.

With this single adjustable parameter fit, the data for the thin film data can be well described, despite the necessary crudity of the assumptions made. However, only in an intermediate temperature range is reasonable agreement obtained for the macroscopic data, the curvature being significantly greater than the model predicts. Several factors may be important here. First, it should be noted that the annealing temperature for the macroscopic samples was some 20°C lower than for the thin film data, although the aging time was kept constant, and so the state of the glass will not be identical. Secondly, no attempt has been made to account for the different specimen geometries, and changes in geometrical constraint may be expected to change the stress for deformation onset. Thirdly, near T_g as well as close to the shear to craze transition some shear is likely to be occurring and this is also likely to complicate the analysis. Despite all these uncertainties it is clear that this approach does provide a reasonable fit, and thus has a predictive capability.

The molecular weight dependence of the crazing stress is also found to be similar in the thin film and the macroscopic data. This can be demonstrated by a similar fitting procedure for M as has been done for $\dot{\epsilon}$. As before, A is used as the fitting parameter. It is found to scale as $M^{-2\pm0.5}$ for both the thin film and macroscopic data, as opposed to the M^{-1} implied by eq. (2c). Currently we are examining the molecular weight dependence in PS. Preliminary results suggest there is good agreement between the model and the observed molecular weight scaling in monodisperse PS in the disentanglement regime. Thus we are led to speculate that the disagreement in the case of PES is due to the very broad molecular weight distributions of our samples. This will be further ex-

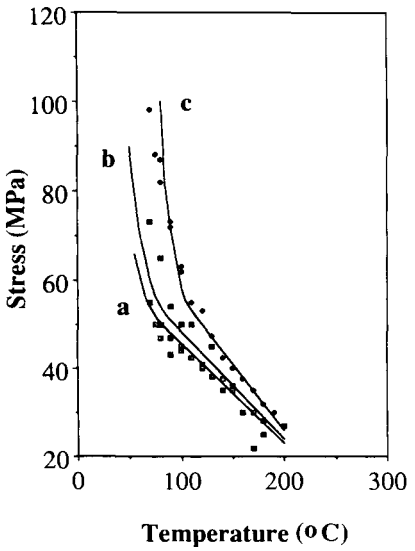

Fig. 10. Empirical fits of eq. (2) to the stress to craze as a function of temperature: (a) in thin films of PES M_w1 at a strain rate of 5×10^{-5} s^{-1}; (b) in macroscopic test bars of PES M_w1 at a strain rate of 2×10^{-4} s^{-1} (fracture stress data); (c) in thin films of PES M_w1 at a strain rate of 10^{-2} s^{-1}.

amined by systematically changing the polydispersity of PS samples. (It is perhaps worth noting that the implication of these fits is that the "transition regime," which we have previously referred to as being dominated by disentanglement,[1] in fact represents a mixed regime of scission and disentanglement.) Hence, it must be concluded that although the results of the macroscopic tests are consistent with the thin film data and the qualitative predictions of the model, we have some way to go towards a complete understanding of the crazing behavior of PES.

CONCLUSIONS

Tensile tests carried out on various molecular weight averages of PES have shown that there is a ductile–brittle transition with increasing temperature. The lowest transition temperatures are for the lowest molecular weight average samples. We have been able to relate this fracture behaviour directly to observations of the deformation behavior of thin films of PES, where we have shown there to be a molecular-weight-dependent transition from shear deformation to crazing with increasing temperature. Assuming that brittle fracture is directly related to the onset of crazing in macroscopic samples, we have shown the behavior of our test bars to be consistent with both the thin film data and the qualitative predictions of a simple model for the transition to disentanglement controlled crazing in PES. This model does not, however, predict the correct molecular weight scaling for the stress to craze in these samples. It is speculated that this is a consequence of the polydispersity of our polymers.

We would like to acknowledge the support of ICI plc during the course of this work, and in particular A. Titterton, for providing data on the molecular weight distributions of our samples, and R. Young, for assisting us with the rheological measurements. We would also like to acknowledge valuable discussions with Professor E. J. Kramer.

References

1. C. J. G. Plummer and A. M. Donald, *J. Polym. Sci. Polym. Phys. Ed.*, **27**, 325 (1989).
2. P. G. DeGennes, *J. Chem. Phys.*, **55**, 572 (1971).
3. M. Doi and S. F. Edwards, *J. Chem. Soc. Far. Trans.*, **74**, 1789, 1802 (1978).
4. T. C. B. McLeish, C. J. G. Plummer, and A. M. Donald, *Polymer*, **30**, 1651 (1989).
5. E. J. Kramer and L. L. Berger, *Adv. Polym. Sci. 91/92*, H. H. Kausch, Ed., Springer-Verlag, Berlin, 1990.
6. E. J. Kramer, *Adv. Polym. Sci. 52/53*, H. H. Kausch, Ed., Springer-Verlag, Berlin, 1983.
7. N. Verheulpen-Heymans, *Polymer*, **20**, 356 (1979).
8. A. M. Donald, *J. Mater. Sci.*, **20**, 2634 (1985).
9. L. L. Berger and E. J. Kramer, *Macromolecules*, **20**, 1980 (1987).
10. S. G. James, PhD Thesis, University of Cambridge, 1988.
11. M. Davies and D. R. Moore, ICI plc. Internal Report, 1987.
12. P. B. Bowden, in *The Physics of Glassy Polymers*, R. N. Haward, Ed., Applied Science, London, 1973.
13. B. D. Lauterwasser and E. J. Kramer, *Phil. Mag.*, **A39**, 469 (1979).
14. L. L. Berger and E. J. Kramer, *J. Mater. Sci.*, **23**, 3536 (1988).
15. J. G. Williams, in *Fracture Mechanics of Polymers*, Ellis Horwood, Chichester, 1984.
16. J. T. Seitz, presented at the 50th Golden Jubilee of the Rheology Society, Boston (1979).
17. G. Allen and J. McAinsh, *Eur. Polym. J.*, **6**, 1635 (1970).

Received October 31, 1989
Accepted November 6, 1989

APPENDIX A

For chain scission, assuming the chain length associated with a scission event to be the bond length a, then the force to break a bond is approximately[5]

$$f_b = \frac{U}{2a} \tag{5}$$

where U is the bond energy. The force acting along a disentangling chain is given by[4]

$$f_d = 2\zeta_0 v (M/M_0) x \tag{6}$$

where v is the craze widening rate, ζ_0 is the monomeric friction coefficient, M_0 is the monomer molecular weight, and x is the fraction of the total length of chain which must disentangle at some fixed point in time in order for the chain to be incorporated into a given fibril. In each case, the effective contribution to the surface tension is given by multiplying the appropriate force by the number of entangled strands per unit length in the surface, which is approximately $\nu_e da/2$ (ν_e is the entanglement density, d is the entanglement separation, and a is the bond length associated with a scission event).[5] Since x in eq. (6) may take any value between 0 and $\frac{1}{2}$, the range of forces necessary for disentanglement may overlap with the force required for chain scission, so that there will be contributions to the surface energy from both. A critical value of x given by

$$x_c = \frac{U}{4a} \frac{M_0}{\zeta_0 v M} \tag{7}$$

may be obtained by equating f_b and f_d. For $x > x_c$, since $f_d > f_b$ we expect a given chain to break rather than disentangle whereas for $x < x_c$ the chain will disentangle. Thus for $x_c < \frac{1}{2}$ we should weight our surface energy contributions accordingly.[5] Denoting the van der Waals surface tension as Γ_0, and the contributions to the overall surface tension Γ from scission and disentanglement as Γ_b and Γ_d, respectively we have

$$\Gamma = \Gamma_0 + \Gamma_b + \Gamma_d = \Gamma_0 + \left(1 - \int_0^{x_c} \phi(x)\, dx\right) \frac{d\nu_e U}{4} + \frac{d\nu_e a}{2} \frac{2\zeta_0 v M}{M_0} \frac{\int_0^{x_c} \phi(x)\, dx \int_0^{x_c} \phi(x) x\, dx}{\int_0^{x_c} \phi(x)\, dx} \tag{8}$$

where $\phi(x)$ is the probability density function for x, which we shall take to be equal to 2 in the range $0 < x \leq \frac{1}{2}$, corresponding to a flat probability distribution. Hence, evaluating the integral, and substituting x_c back into the expression for Γ_d using eq. (7), we obtain for $x_c < \frac{1}{2}$

$$\Gamma = \Gamma_0 + (1 - 2x_c) \frac{d\nu_e U}{4} + x_c \frac{d\nu_e U}{4} \tag{9}$$

and similarly, where $x_c \geq \frac{1}{2}$ (no scission)

$$\Gamma = \Gamma_0 + \frac{d\nu_e a}{2} \frac{2\zeta_0 v M}{M_0} \left(\frac{1}{4}\right) = \Gamma_0 + \frac{d\nu_e U}{4} \frac{1}{4x_c} \tag{10}$$

[Physically, of course, $x_c = \frac{1}{2}$ is the limiting case although x_c in eq. (7) may be greater than $\frac{1}{2}$.]

Hence we have that the crazing stress S_c is given by

$$S_c \sim \left(\Gamma_0 + (1 - x_c) \frac{d\nu_e U}{4}\right)^{1/2}, \qquad \frac{1}{2} > x_c \tag{11a}$$

$$S_c \sim \left(\Gamma_0 + \frac{1}{4x_c}\frac{d\nu_e U}{4}\right)^{1/2}, \qquad \frac{1}{2} \leq x_c \tag{11b}$$

where

$$x_c = \frac{U}{4a}\frac{M_0}{\zeta_0 \upsilon M} \tag{11c}$$

APPENDIX B

Three grades of PES were investigated; M_w1, M_w3, and M_w4. Sections from the ends of the macroscopic test bars were placed in the rheometer (Rheometrics Dynamic Spectrometer 7700) and pressed into a suitable test geometry at approximately 300°C (the resulting plaques were approximately 1.7 mm thick, compared with a starting thickness of about 3.2 mm).

The entanglement molecular weight M_e of the PES was determined using the method of Seitz.[16] Temperature scans at a constant displacement rate of 0.6 rad s^{-1} and maximum displacement of 0.8 rad were carried out to determine the position of the minimum in tan δ as a function of T. The results are as follows:

Grade	T (°C)
M_w1	241
M_w3	242
M_w4	243

(The maximum resolution on the temperature axis was 1°C.)

Owing to difficulties with grip slip, frequency scans were done at the slightly higher temperature of 245°C. The values obtained for the plateau modulus G'_0 and the entanglement molecular weight M_e were as follows:

Grade	G'_0 (GPa)	M_e
M_w1	3.43	1630
M_w3	3.5	1605
M_w4	3.7	1518

The values of M_e were obtained using $M_e = 10^3 \rho R T_0 / G'_0$, where T_0 is the measurement temperature and the density ρ was taken to be 1310 kg m^{-3} at 245°C. The mean bond length is 5.87 Å; the value $\langle r^2 \rangle / N$ is approximately 75×10^{-20} m^2, where N is the number of bonds in the length of polymer under consideration.[17] Taking M_e to be 1600, we have that there are approximately 14 bonds (each consisting of a phenyl group separating SO_2 and O) between entanglement points. Thus, the rms entanglement point separation is approximately 32 Å. The contour length may be estimated by assuming the bond angles to be approximately 109.5° leading to a value of 48 Å. Thus λ_{max}, the ratio of these two quantities, is predicted to be 1.5.

A calculation of $6 \times 10^{26}\ \rho / M_e$ gives ν_e to be 50×10^{25} m^{-3} at 245°C and a value of 52×10^{25} m^{-3} at 20°C, allowing for the variation of ρ with T.